ACS APPLIED MATERIALS & INTERFACES

Letter

www.acsami.org

Grazing Incidence Cross-Sectioning of Thin-Film Solar Cells via Cryogenic Focused Ion Beam: A Case Study on CIGSe

Kasra Sardashti,[†] Richard Haight,[‡] Ryan Anderson,[§] Miguel Contreras,[∥] Bernd Fruhberger,[§] and Andrew C. Kummel*[,†]

[†]Department of Chemistry and Biochemistry, University of California San Diego, La Jolla, California 92093−0358, United States

[‡]IBM TJ Watson Research Center, Yorktown Heights, New York 10598, United States

[§]California Institute for Telecommunications and Information Technology, University of California San Diego, La Jolla, California 92093-0436, United States

[∥]National Renewable Energy Laboratory, Golden, Colorado 80401, United States

Supporting Information

ABSTRACT: Cryogenic focused ion beam (Cryo-FIB) milling at near-grazing angles is employed to fabricate cross-sections on thin Cu(In,Ga)Se_2 with >8x expansion in thickness. Kelvin probe force microscopy (KPFM) on sloped cross sections showed reduction in grain boundaries potential deeper into the film. Cryo Fib-KPFM enabled the first determination of the electronic structure of the Mo/CIGSe back contact, where a sub 100 nm thick $MoSe_y$ assists hole extraction due to 45 meV higher work function. This demonstrates that CryoFIB-KPFM combination can reveal new targets of opportunity for improvement in thin-films photovoltaics such as high-work-function contacts to facilitate hole extraction through the back interface of CIGS.

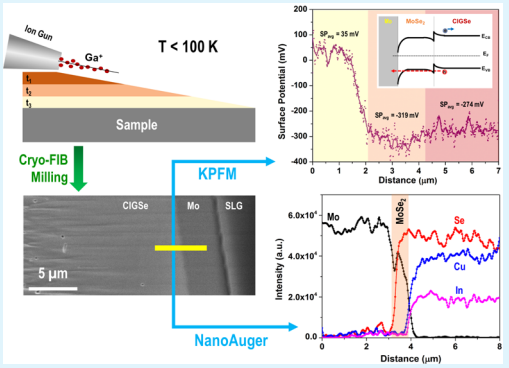

KEYWORDS: *thin-film photovoltaics, Cryo-FIB, KPFM, CIGSe, back contacts*

Photovoltaics (PV) is a fast-growing source of renewable energy and is projected to gain more than 11% of the global electricity market by 2050.[1] To become more competitive with the current sources of electricity, it is crucial to reduce the cost per watt generated power by lowering the manufacturing costs and increasing the conversion efficiencies.[2] This can be achieved by the use of thin-film PV technologies such as CdTe and Cu(In,Ga)Se_2 (CIGSe), where the overall materials consumption is lowered by reducing the film thickness to less than 5 μm.[3] In addition, relatively simple growth techniques for thin films enable large-area monolithic manufacturing of the modules. In order to reaching the goal of few TW/year power generation,[4] in addition to CdTe and CIGSe which have achieved record cell efficiencies above 20%, other earth-abundant thin film alternatives such as $Cu_2ZnSn(S,Se)_4$ (CZTSSe) and the perovskite family ($MAPbI_3$ in particular) are being explored.[4,5]

The wide majority of thin film absorbers are polycrystalline with a large density of grain boundaries. Grain boundaries, if not properly passivated, could be detrimental to the device performance of solar cells by accommodating a large density of recombination sites.[6] In addition, thin film devices are composed of multiple layers of materials (i.e., absorbers, buffers, contacts, etc.) with heterojunctions that are required to have low defect density. Therefore, it is essential to employ low damage techniques to measure the composition and electrical properties of the grain boundaries and interfaces in thin film PV device. Specifically, measurements of composition and charge distribution in the cross sections of the devices via energy-dispersive X-ray spectroscopy (EDX), Auger nanoprobe microscopy (Nano-Auger) and scanning probe microscopy (SPM) can correlate the device performance with the chemistry and physics of the interfaces within the device.[7] However, unlike single-crystalline materials (Si, GaAs, etc.), preparation of flat cross-sections by single-step cleaving is challenging for thin films solar devices, since fracture in polycrystalline materials mostly occurs along the grain boundaries.[7,8] Consequently, smooth cross-sections for polycrystalline absorbers are only achieved after additional processing steps following the cleaving such as chemical-mechanical or mechanical polishing and ion milling.[9−11] In addition to increase in processing complexity, these additional steps potentially induce mechanical damage in the sample and make the cross-sectional measurements rather unrepresentative.

In the present report, an alternative method is proposed for preparation of smooth cross sections for thin film solar cell absorbers by using cryogenic focused ion beam (Cryo-FIB) milling with near grazing angles of incidence of the Ga^+ ion beam. Successful application of this technique in characterization of

Received: April 8, 2016
Accepted: June 1, 2016

DOI: 10.1021/acsami.6b04214
ACS Appl. Mater. Interfaces XXXX, XXX, XXX−XXX

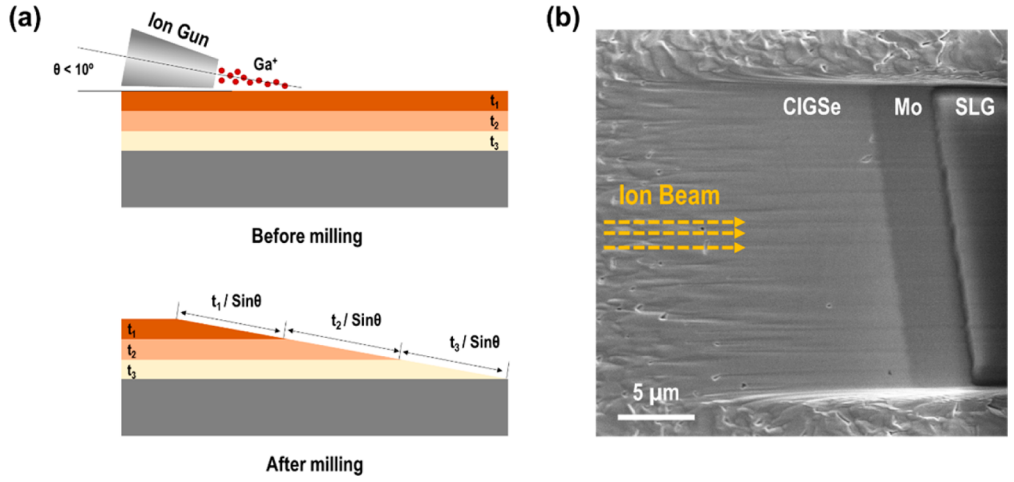

Figure 1. Cryo-FIB cross-sectioning procedure: (a) Schematic showing the process of grazing incidence cross-sectioning of multilayer thin film substrates by focused ion beam (FIB). The parameter θ is the angle between the incoming beam and sample surface which was varied between 5 and 8° depending on the required amount of scale expansion. The thickness of each layer exposed by grazing incidence milling is proportional to $1/\sin\theta$. (b) SEM micrograph of a cross-section milled using a grazing ion beam incidence angle of 5° on a CIGSe film (bright top surface) grown on Mo-coated soda lime glass (SLG).

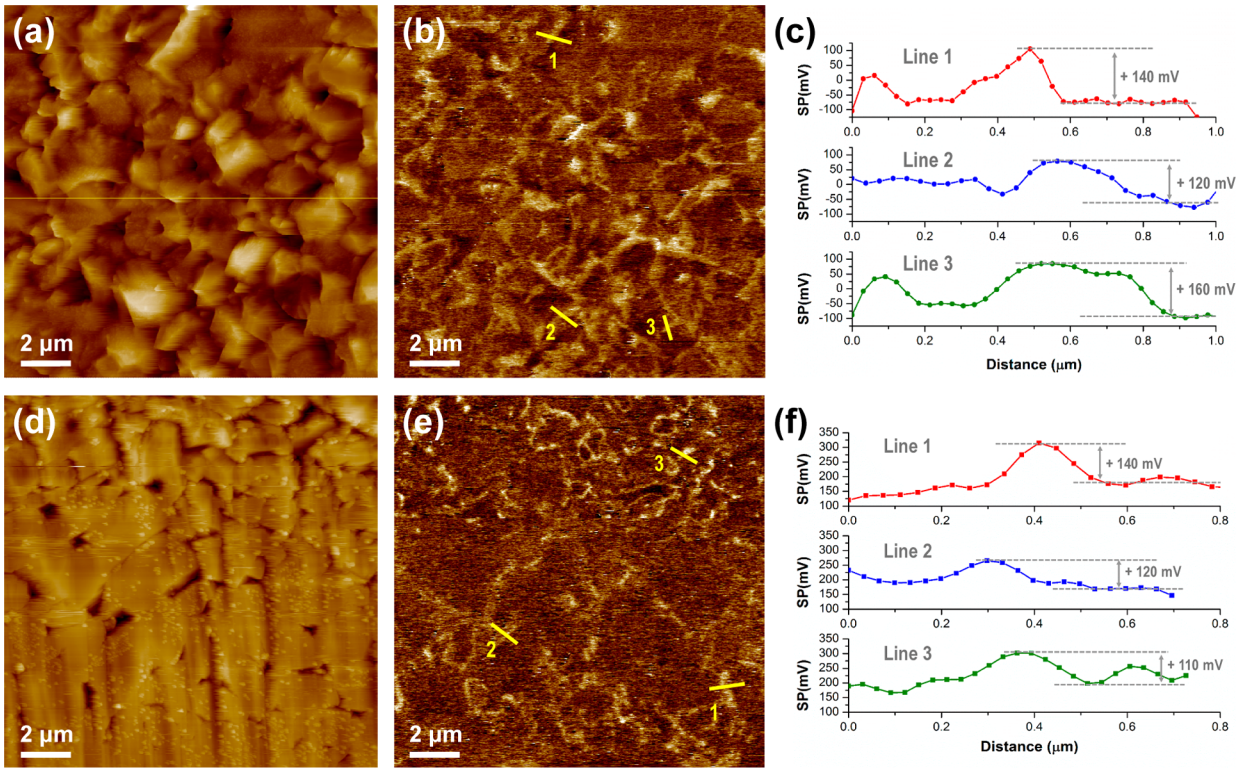

Figure 2. Topography and surface potential maps in planar and cross-sectional geometries: (a, b) Planar topography and surface potential maps for clean a CIGSe surface recorded simultaneously during the Kelvin probe force microscopy (KPFM) measurements. Scan size is 15 μm × 15 μm. (c) Line traces for surface potential in three different locations shown by yellow lines in b. The yellow bars specify the locations of the grain boundaries where the line traces were measured. (d, e) Topography and surface potential maps measured on sloped cross sections milled with the incidence angle of 5°. Measurements were carried out on the upper half of the cross-section to exclude the Mo/CIGSe interface. Scan size is 15 μm × 15 μm. (f) Line traces for topography and surface potential lines shown by yellow lines in e. The yellow bars specify the locations of the grain boundaries where the line traces were measured.

grain boundaries and back contacts in CIGSe absorbers is demonstrated. Grazing incidence ion beam angles are beneficial in reducing the Ga^+ implantation during the milling process by shrinking the ion−surface interaction cascade's effective volume.[12,13] Moreover, because the sample is cooled to cryogenic temperatures (80−100 K), local ion beam heating and Ga^+ ion diffusion within the bulk of the films are expected to be significantly suppressed.[14,15] Therefore, this combination ensures minimal beam damage and Ga^+ incorporation during the milling procedure of sloped cross-sections.

Figure 1a shows a schematic of the grazing incidence Cryo-FIB cross-sectioning process for a multilayer solar cell stack. It also

DOI: 10.1021/acsami.6b04214
ACS Appl. Mater. Interfaces XXXX, XXX, XXX−XXX

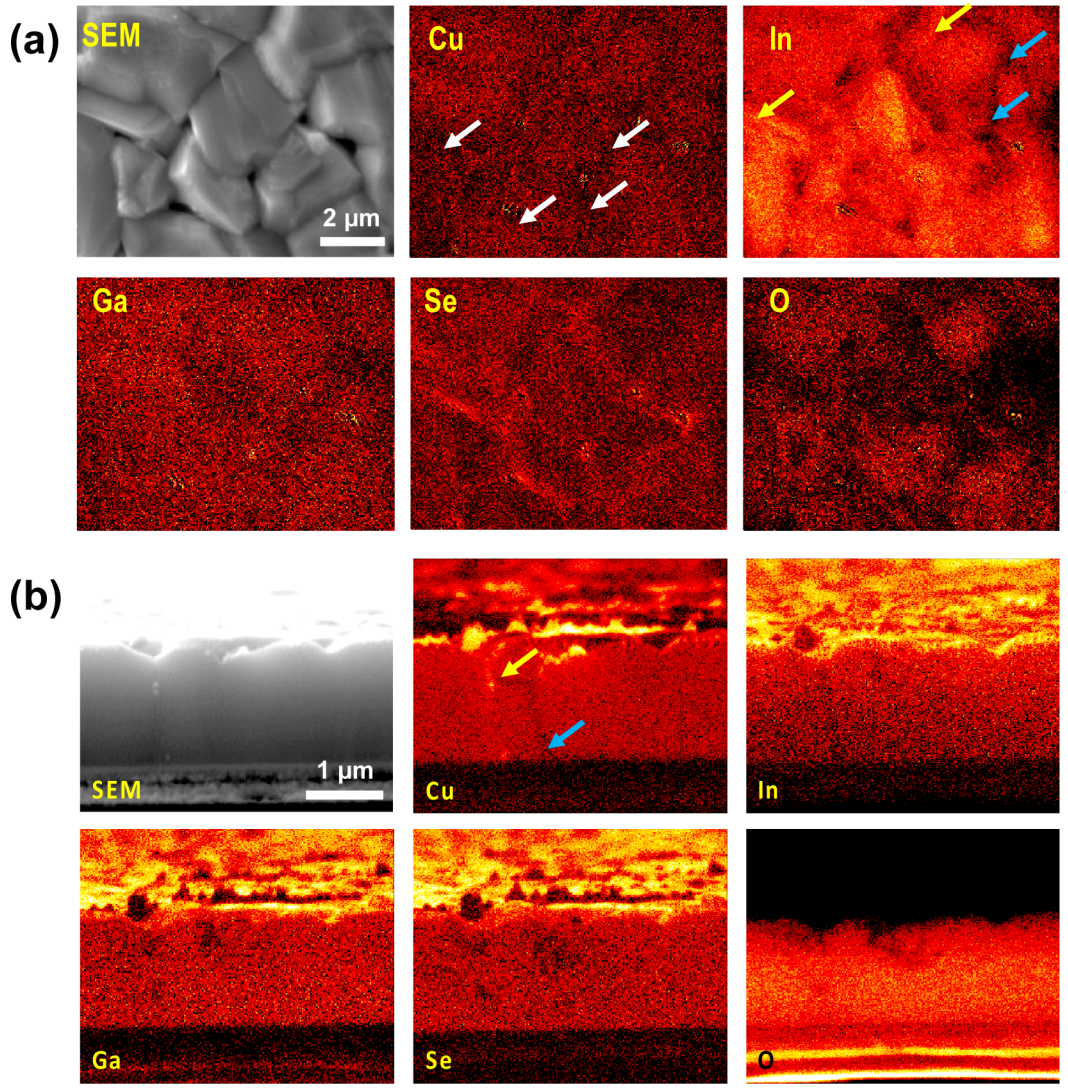

Figure 3. NanoAuger elemental maps for CIGS in planar and cross-sectional geometry: (a) planar SEM micrograph and NanoAuger elemental maps for Cu, In, Ga, Se, and O for clean CIGSe surface. The nonuniformity in the elemental maps does not correspond to the grain boundaries but to the grain top surfaces. (b) Cross-sectional SEM micrograph and NanoAuger elemental maps for Cu, In, Ga, Se, and O measured on surfaces prepared by normal incidence Cryo-FIB. Two of the vertical grain boundaries appear to be Cu-rich near the top (yellow arrow) and Cu-poor near the bottom (blue arrow) of the CIGSe film.

outlines another important advantage of milling with grazing incidence angles: scale expansion. The thickness probed from each layer is proportional to the cosecant of θ (angle between Ga^+ ion beam and sample surface, cosec $\theta = 1/\sin\theta$). Therefore, considering $\theta < 10°$, the lateral scale can be expanded between 7.2 and 11.5 times. A SEM micrograph of a sloped cross-section milled with 5° incidence ion beam angle, on a 2 μm thick CIGSe ([Ga]/[In]+[Ga] = 0.3) absorber layer deposited on Mo-coated soda lime glass (SLG) is shown in Figure 1b. Details of CIGSe thin film growth and PV performance are given in the Supporting Information. Milling the sloped cross-section was achieved in two steps: (1) Bulk milling where a 30 kV, 3 nA beam is used for quick removal of the film and back contact layer; (2) fine milling where a 5 kV, 48−77 pA beam is used to remove the damaged layer formed near the top surface. The total milling time for the two steps is less than 20 min. It should be noted the streaks expanding from the CIGSe top surface to the bottom Mo/glass interface were caused by the "curtaining effect"; an effect known to be caused by orientation induced sputter rate variations due to ion channeling.[16,17] However, the roughness level resulting from the curtaining is less than 10 nm (RMS roughness ~6.7 nm) which is much lower than what is typically measured on CIGSe films top surfaces (about 100−200 nm). Therefore, the cross-sections have sufficiently smooth surfaces that are ideal for scanning probe measurements where cross-talk between electrical and topographical signals is a concern.[18]

Kelvin probe force microscopy (KPFM) was employed to determine the surface potential (or contact potential difference) variations across the grain boundaries on both the top surface and within the sloped cross sections. KPFM measurements were performed using a dual lock-in amplifier configuration in which topography and surface potential are measured simultaneously with minimal cross-talk (details of experimental setup are given in the Supporting Information). Figure 2a, b shows the topography and surface potential maps measured simultaneously on top surfaces of bare CIGSe films. To minimize oxidation of clean surfaces during the measurements, we continuously purged the atomic force microscope (AFM) chamber by high purity Ar gas. By correlating the two maps, it becomes evident that the majority of the grain boundaries have more positive charge

DOI: 10.1021/acsami.6b04214
ACS Appl. Mater. Interfaces XXXX, XXX, XXX−XXX

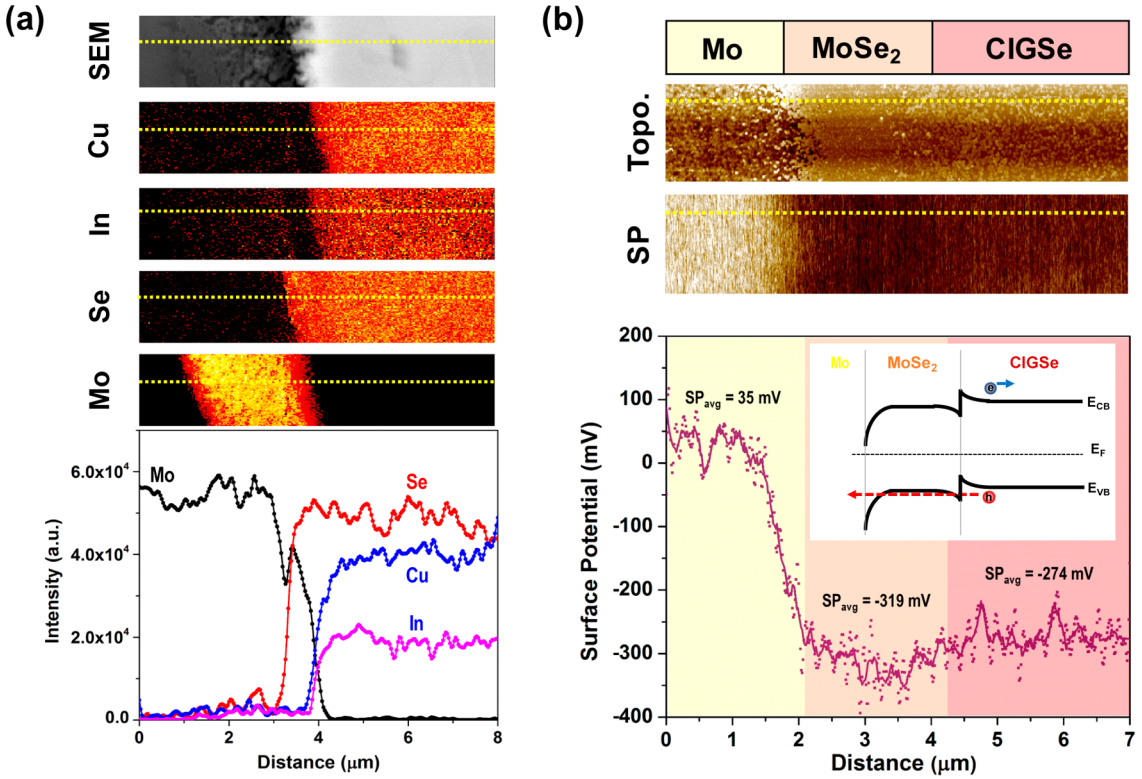

Figure 4. NanoAuger and KPFM Measurements on CIGSe/Mo Back Interface: (a) SEM micrograph and NanoAuger elemental maps for Cu, In, Se, and Mo for a CIGSe sloped cross-section prepared by Cryo-FIB milling at 8° ion beam incidence angle. The Mo and Se maps show an area of overlap which is the $MoSe_y$. Line traces confirm the presence of a $MoSe_y$ layer between Mo and Se in CIGSe. (b) Topography and surface potential measurements performed on the CIGSe sample with 5° ion beam incidence angle, showing a small potential drop across the interface between Mo and CIGSe that corroborates the presence of $MoSe_y$.

relative to the grains. These results are consistent with the previous reports on planar KPFM measurements of CIGSe where positive charge (or downward band bending) of about 100−200 mV was measured at the grain boundaries.[19,20] On the top surface, the amount of band bending at the grain boundaries varies between 120 and 160 mV, as shown by surface potential line traces in Figure 2c. These lines traces were taken from three different locations in the surface potential map, marked by yellow lines, where grain boundaries exist.

Figure 2d, e display the topography and surface potential maps, measured under Ar, on CIGSe sloped cross-sections milled using a 5° ion beam incidence angle. This cross-section was prepared under the same condition as the one shown in Figure 1b. Similar to planar KPFM measurements, positively charged grain boundaries are observed from the top to the bottom of the 15 × 15 μm^2 scan area. The surface potential line traces shown in Figure 2f, confirm that the extent of downward band bending varies between 110 and 140 mV. Therefore, grain boundaries maintained the same charge polarity as the top surface after Cryo-FIB milling, consistent with minimal ion beam damage to the electronic structure. There is also 40−50 meV reduction in the amount of band bending from the top to the bottom of the scan area (Figure S1) consistent with the 3D models proposed for CIGSe where grain boundary band bending is combined with the upward band bending of individual grains due to Cu-depleted top surfaces.[20] Smaller band bending at the grain boundaries deeper into the film might increase the overall grain boundary recombination. Therefore, Cryo-FIB milling at grazing ion beam incidence angles can be a strong tool for preparing smooth surfaces on which variation of grain boundary potential as a function of depth can be investigated to determine targets of opportunity for PV performance improvement.

The downward band bending at the grain boundaries of low Ga content CIGSe thin films has been attributed to a number of factors including Cu-depletion as well as Na accumulation adjacent to the grain boundaries.[21,22] Na can either diffuse from the soda lime glass (SLG) substrate into the grain boundaries or be intentionally added as a layer of NaF. To determine the grain boundary composition, we performed planar and cross-sectional NanoAuger measurements on CIGSe films. Figure 3a displays the SEM micrograph and NanoAuger elemental maps for Cu, In, Ga, Se, and O in planar mode on CIGSe surfaces. The surface oxide was removed by immersion in NH_4OH for 15 min followed by a short rinse in DI water. Grain boundaries in CIGSe appear to vary in composition with some regions being In-poor (blue arrows) and some In-rich (yellow arrows). Moreover, some fraction of grain boundaries appears to be slightly Cu-poor (white arrows). The Ga map is slightly nonuniform, and the majority of Ga depletion occurs on the top surfaces of the grains. Unlike the elemental maps for CZTSSe, where a uniform layer of SnO_x is observed at grain boundaries (Figure S2),[7] for CIGSe films O distribution is quite nonuniform and O-rich regions are divided in between the grain surfaces and grain boundaries. Therefore, the downward band bending cannot be attributed to a distinct grain boundary composition visible within the Nano-Auger resolution limit (∼8 nm).

Figure 3b shows cross-sectional NanoAuger measurements on the vertical cross sections prepared by Cryo-FIB with 90° ion beam incidence angle. The milling parameter for bulk and fine milling were 30 kV, 3 nA and 5 kV, 77 pA, respectively. In this flat

DOI: 10.1021/acsami.6b04214
ACS Appl. Mater. Interfaces XXXX, XXX, XXX−XXX

cross-section, two vertical grain boundaries are visible near the left-hand side of the images. The tops of these grain boundaries are covered with some Cu-rich features (yellow arrow) which could be formed as a result of CIGSe resputtering during the milling process. However, near the bottom, these grain boundaries appear to be Cu-poor (blue arrow) consistent with results suggested by atom probe tomography, etc.[21] Therefore, at least in the few grain boundaries captured by NanoAuger mapping, Cu depletion occurs which could lead to lower work function and downward band bending.

Beside characterization of grain boundaries deeper within the polycrystalline films, FIB cross-sectioning with grazing incidence angle has been used to characterize the interface between Mo and CIGSe near the backside. Figure 4a shows the SEM micrograph and NanoAuger elemental maps for Cu, In, Se and Mo for a 1×8 μm^2 section of CIGSe/Mo back contact interface. These NanoAuger measurements were performed on a sloped cross-section milled with the incidence angle of 8°. The maps and line scans at the bottom of the figure (Mo, Se, In, and Ga lines) demonstrate that there is an overlap region between the Mo and Se signals, highlighted by pale orange, consistent with formation of a thin layer of $MoSe_y$ between Mo and CIGSe. The Mo/Se ratio determined by single point Auger spectroscopy is about 1 ($y \approx 1$). This layer is believed to grow during the selenization process of the CIGSe films, where Se gas is introduced into the growth chamber in order to react with metallic components deposited on the Mo film. However, Mo would also react with Se to form a thin layer of $MoSe_y$.[23,24]

Although the presence of $MoSe_y$ between Mo and CIGSe has been previously determined by chemical composition measurements such as TEM-EELS and XPS,[23,25] little is known about the electrical potential variations across the CIGSe/$MoSe_y$/Mo interfaces. To determine the electronic structure of these interfaces, KPFM measurements were performed under an Ar environment on a sloped cross-section milled at 5° ion beam incidence angle. A smaller ion beam incidence angle was chosen in order to further expand the scale since minimum resolution for KPFM measurements (>20−30 nm) is at least three times larger than NanoAuger (~8 nm). Topography and surface potential maps measured by cross-sectional KPFM are shown in Figure 4b. The KPFM images show a region between Mo and CIGSe with slightly lower potential ($\Delta(SP)_{avg} \approx 45$ mV) than CIGSe. Therefore, based on the KPFM fundamental equation ($SP = \varphi_{tip} - \varphi_{sample}/e$),[18] the $MoSe_y$ layer has a 45 meV higher work function than CIGSe. Due to the larger work function, $MoSe_y$ induces upward band bending within the CIGSe close to the back interface, thereby assisting hole extraction from the film. On the basis of work function difference, as well as theoretical predictions on the back surface band diagram,[25] the band structure shown in the inset of Figure 4b has been proposed. However, the resulting upward band bending near the back surface can be too small for maximal hole extraction, necessitating application of back contacts with higher work functions like MoO_x and WO_x. In addition, there is about 350 mV downward band bending within the $MoSe_y$ because of its large difference in work function with Mo. Because the $MoSe_y$ actual thickness is few tens of nanometers, it is predicted that despite downward band bending, holes are able to tunnel from the CIGSe back surface to the Mo contact.[26,27] It should be noted that the actual work function for Mo is lower than the values measured by KPFM. The reason for this difference is oxidation of Mo after Cryo-FIB and its chemical resistance to NH_4OH, which was used to remove the oxide from the CIGSe top surfaces.

In summary, Cryo-FIB milling at grazing incidence angles was employed to prepare smooth cross sections with scale expansions of 7.5−11.5×. KPFM measurements showed little or no change to the grain boundary polarity on these cross-section as a result of ion beam milling. In the cross sections, positively charged grain boundaries are observed from the top to the bottom with downward band bending varying from 140 mV to 75 mV from the top to the bottom. Additionally, this cross-sectioning method enabled the first direct determination of the composition and the electronic structure of the Mo/CIGSe back contact, where a thin layer of $MoSe_y$ was detected by both Auger Nanoprobe and KPFM. Due to 45 meV larger work function than CIGSe, $MoSe_y$ formation can be beneficial in hole extraction by inducing upward band bending in the CIGSe back surface. Hole extraction is expected to improve by the application of high-work-function contact materials such as MoO_x. This cross-sectioning method with minimal processing steps can be beneficial in characterizing various interfaces in multilayer thin film solar cell stacks particularly for sensitive films such as hybrid inorganic−organic perovskites and organic solar cells as well as other inorganic thin films such as CdTe and CZTSSe; this enables identification of targets of opportunity for improvements of PV beyond bulk defects.

■ ASSOCIATED CONTENT

Supporting Information

The Supporting Information is available free of charge on the ACS Publications website at DOI: 10.1021/acsami.6b04214.

Experimental details including CIGSe growth and solar cell characterization, Cryo-FIB milling, KPFM measurements, and NanoAuger elemental mapping; variation in average grain boundary surface potential versus depth for CIGSe cross-section; (c) planar NanoAuger elemental maps for CZTSSe films (PDF)

■ AUTHOR INFORMATION

Corresponding Author

*E-mail: akummel@ucsd.edu.

Notes

The authors declare no competing financial interest.

■ ACKNOWLEDGMENTS

The information, data, or work presented herein was funded in part by the U.S. Department of Energy, Energy Efficiency and Renewable Energy Program, under Award DE-EE0006334. Stanford Nano Shared Facilities are acknowledged for NanoAuger measurements. K.S. thanks Chuck Hitzman for assistance with NanoAuger measurements. Funding for the technique development was also provided by National Science Foundation Grant DMR 1207213.

■ REFERENCES

(1) Candelise, C.; Speirs, J. F.; Gross, R. J. K. Materials Availability for Thin Film (TF) PV Technologies Development: A Real Concern? *Renewable Sustainable Energy Rev.* **2011**, *15* (9), 4972−4981.

(2) Chopra, K. L.; Paulson, P. D.; Dutta, V. Thin-Film Solar Cells: An Overview. *Prog. Photovoltaics* **2004**, *12* (2−3), 69−92.

(3) Aberle, A. G. Thin-Film Solar Cells. *Thin Solid Films* **2009**, *517* (17), 4706−4710.

(4) Mitzi, D. B.; Gunawan, O.; Todorov, T. K.; Wang, K.; Guha, S. The Path Towards A High-Performance Solution-Processed Kesterite Solar Cell. *Sol. Energy Mater. Sol. Cells* **2011**, *95* (6), 1421−1436.

DOI: 10.1021/acsami.6b04214
ACS Appl. Mater. Interfaces XXXX, XXX, XXX−XXX

(5) Gratzel, M. The light and shade of perovskite solar cells. *Nat. Mater.* **2014**, *13* (9), 838−842.
(6) Qiu, Y.; Kunz, O.; Fejfar, A.; Ledinsky, M.; Chan, B. T.; Gordon, I.; Van Gestel, D.; Venkatachalm, S.; Egan, R. On The Effects Of Hydrogenation Of Thin Film Polycrystalline Silicon: A Key Factor To Improve Heterojunction Solar Cells. *Sol. Energy Mater. Sol. Cells* **2014**, *122*, 31−39.
(7) Sardashti, K.; Haight, R.; Gokmen, T.; Wang, W.; Chang, L. Y.; Mitzi, D. B.; Kummel, A. C. Impact of Nanoscale Elemental Distribution in High-Performance Kesterite Solar Cells. *Adv. Energy Mater.* **2015**, *5* (10), 1402180.
(8) Ballif, C.; Moutinho, H. R.; Hasoon, F. S.; Dhere, R. G.; Al-Jassim, M. M. Cross-Sectional Atomic Force Microscopy Imaging of Polycrystalline Thin Films. *Ultramicroscopy* **2000**, *85* (2), 61−71.
(9) Ballif, C.; Moutinho, H. R.; Al-Jassim, M. M. Cross-Sectional Electrostatic Force Microscopy of Thin-Film Solar Cells. *J. Appl. Phys.* **2001**, *89* (2), 1418−1424.
(10) Glatzel, T.; Marron, D. F.; Schedel-Niedrig, T.; Sadewasser, S.; Lux-Steiner, M. C. CuGaSe2 Solar Cell Cross Section Studied by Kelvin Probe Force Microscopy in Ultrahigh Vacuum. *Appl. Phys. Lett.* **2002**, *81* (11), 2017−2019.
(11) Glatzel, T.; Steigert, H.; Sadewasser, S.; Klenk, R.; Lux-Steiner, M. C. Potential Distribution of Cu(In,Ga)(S,Se)(2) Solar Cell Cross-sections Measured by Kelvin Probe Force Microscopy. *Thin Solid Films* **2005**, *480*, 177−182.
(12) Ishitani, T.; Umemura, K.; Ohnishi, T.; Yaguchi, T.; Kamino, T. Improvements in Performance of Focused Ion Beam Cross-Sectioning: Aspects of Ion-Sample Interaction. *J. Electron Microsc.* **2004**, *53* (5), 443−449.
(13) Matteson, T. L.; Schwarz, S. W.; Houge, E. C.; Kempshall, B. W.; Giannuzzi, L. A. Electron Backscattering Diffraction Investigation of Focused Ion Beam Surfaces. *J. Electron. Mater.* **2002**, *31* (1), 33−39.
(14) Kim, S.; Park, M. J.; Balsara, N. P.; Liu, G.; Minor, A. M. Minimization of Focused Ion Beam Damage in Nanostructured Polymer Thin Films. *Ultramicroscopy* **2011**, *111* (3), 191−199.
(15) Orthacker, A.; Schmied, R.; Chernev, B.; Froch, J. E.; Winkler, R.; Hobisch, J.; Trimmel, G.; Plank, H. Chemical Degradation and Morphological Instabilities During Focused Ion Beam Prototyping of Polymers. *Phys. Chem. Chem. Phys.* **2014**, *16* (4), 1658−1666.
(16) Munroe, P. R. The Application of Focused Ion Beam Microscopy in The Material Sciences. *Mater. Charact.* **2009**, *60* (1), 2−13.
(17) Phaneuf, M. W., FIB for Materials Science Applications−a Review. In *Introduction to Focused Ion Beams: Instrumentation, Theory, Techniques and Practice*p; Giannuzzi, L. A.; Stevie, F. A., Eds.; Springer: Boston, 2005; pp 143−172.
(18) Melitz, W.; Shen, J.; Kummel, A. C.; Lee, S. Kelvin Probe Force Microscopy and Its Application. *Surf. Sci. Rep.* **2011**, *66* (1), 1−27.
(19) Jiang, C. S.; Contreras, M. A.; Repins, I.; Moutinho, H. R.; Yan, Y.; Romero, M. J.; Mansfield, L. M.; Noufi, R.; Al-Jassim, M. M. How Grain Boundaries in Cu(In,Ga)Se-2 Thin Films Are Charged: Revisit. *Appl. Phys. Lett.* **2012**, *101* (3), 033903.
(20) Jiang, C. S.; Repins, I. L.; Mansfield, L. M.; Contreras, M. A.; Moutinho, H. R.; Ramanathan, K.; Noufi, R.; Al-Jassim, M. M. Electrical Conduction Channel Along The Grain Boundaries of Cu(In,Ga)Se2 Thin Films. *Appl. Phys. Lett.* **2013**, *102* (25), 253905.
(21) Abou-Ras, D.; Schmidt, S. S.; Caballero, R.; Unold, T.; Schock, H. W.; Koch, C. T.; Schaffer, B.; Schaffer, M.; Choi, P. P.; Cojocaru-Miredin, O. Confined and Chemically Flexible Grain Boundaries in Polycrystalline Compound Semiconductors. *Adv. Energy Mater.* **2012**, *2* (8), 992−998.
(22) Raghuwanshi, M.; Cadel, E.; Pareige, P.; Duguay, S.; Couzinie-Devy, F.; Arzel, L.; Barreau, N. Influence of Grain Boundary Modification on Limited Performance of Wide Bandgap Cu(In,Ga)Se2 Solar Cells. *Appl. Phys. Lett.* **2014**, *105* (1), 013902.
(23) Yoon, J. H.; Park, J. K.; Kim, W. M.; Lee, J.; Pak, H.; Jeong, J. H. Characterization of Efficiency-Limiting Resistance Losses in Monolithically Integrated Cu(In,Ga)Se2 Solar Modules. *Sci. Rep.* **2015**, *5*, 7690.
(24) Weinhardt, L.; Blum, M.; Bar, M.; Heske, C.; Fuchs, O.; Umbach, E.; Denlinger, J. D.; Ramanathan, K.; Noufi, R. Chemical Properties of The Cu(In,Ga)Se2/Mo/Glass Interfaces in Thin Film Solar Cells. *Thin Solid Films* **2007**, *515* (15), 6119−6122.
(25) Caballero, R.; Nichterwitz, M.; Steigert, A.; Eicke, A.; Lauermann, I.; Schock, H. W.; Kaufmann, C. A. Impact of Na On MoSe2 Formation at The CIGSe/Mo Interface in Thin-Film Solar Cells on Polyimide Foil at Low Process Temperatures. *Acta Mater.* **2014**, *63*, 54−62.
(26) Chirila, A.; Buecheler, S.; Pianezzi, F.; Bloesch, P.; Gretener, C.; Uhl, A. R.; Fella, C.; Kranz, L.; Perrenoud, J.; Seyrling, S.; Verma, R.; Nishiwaki, S.; Romanyuk, Y. E.; Bilger, G.; Tiwari, A. N. Highly Efficient Cu(In,Ga)Se-2 Solar Cells Grown on Flexible Polymer Films. *Nat. Mater.* **2011**, *10* (11), 857−861.
(27) Hsiao, K. J.; Liu, J. D.; Hsieh, H. H.; Jiang, T. S. Electrical Impact of MoSe2 on CIGS Thin-Film Solar Cells. *Phys. Chem. Chem. Phys.* **2013**, *15* (41), 18174−18178.

DOI: 10.1021/acsami.6b04214
ACS Appl. Mater. Interfaces XXXX, XXX, XXX−XXX